

Proceedings of the Korean Nuclear Spring Meeting  
Gyeongju, Korea, May 2003

## Interdiffusion Reaction Layer Growth Behavior of U-Mo/Al Dispersion Fuels

Ho Jin Ryu, Young Soo Han, Jong Man Park, Soon Dal Park, and Chang Kyu Kim

Korea Atomic Energy Research Institute  
150 Deokjin-dong, Yuseong-gu, Daejeon 305-353, Korea

### Abstract

The growth behavior of reaction layers during the reaction between U-Mo powders and the Al matrix in U-Mo/Al dispersion fuels were investigated. Annealing of 10vol% U-10Mo/Al dispersion fuels at temperatures from 500°C to 550°C was carried out for 10 min - 36 hrs to measure the growth rate and the activation energy for the growth of reaction layers. The concentration profiles of reaction layers between the U-10Mo vs. Al diffusion couples were measured and the integrated interdiffusion coefficients were calculated for the U and Al in the reaction layers.

### 1. Introduction

The international research reactor community has decided to use low-enriched uranium (LEU) instead of highly enriched uranium (HEU) according to the non-proliferation policy under the reduced enrichment for research and test reactors (RERTR) program. Uranium silicide dispersion fuels such as  $U_3Si_2/Al$  and  $U_3Si/Al$  are being used in research reactors due to their stable irradiation behavior. However, high uranium density dispersion fuels (8-9 g/cm<sup>3</sup>) are required for some high performance research reactors[1,2]. Since uranium compounds cannot meet the density requirements except for  $U_6Fe$  and  $U_6Mn$  which have shown poor irradiation behavior, uranium alloys with high uranium density have been studied for their possible use in research reactors[3]. U-Mo alloys have been considered as one of the most promising uranium alloys for a dispersion fuel due to the good irradiation performance of its cubic uranium phase. It is also known that reprocessing of uranium silicide dispersion fuels is difficult[4], whereas the U-Mo dispersion fuel was considered to be reprocessable[5]. In connection with the end of the US return policy in 2006, an accelerated qualification program to replace the uranium silicide dispersion fuel with U-Mo dispersion fuel was undertaken by the RERTR program[6].

U-Mo dispersion fuels for research reactors have been prepared by rolling or extruding the blended powders of U-Mo alloys and aluminum[7]. U-Mo powders are conventionally supplied by the mechanical comminution of as-cast U-Mo alloys. In order to simplify the preparation process and improve the properties, a rotating-disk centrifugal atomization

method has been developed[8]. The centrifugally atomized powders have some advantages that the powder has a rapidly solidified  $\gamma$  uranium structure, a relatively narrow particle size distribution, and a spherical shape[9].

In dispersion fuels, dimensional and geometric changes occur as a result of interdiffusion or chemical reactions between fuel particles and the matrix[10]. The volume expansion produced by thermal annealing is thus a measure of the thermal stability of the dispersion fuels, and it is regarded as an indicator of expected in-reactor swelling performance. In the case of U-Mo/Al dispersion fuel, U-Mo powders and the Al matrix react to form intermetallic compounds which are less dense than the combined reactants, when it is annealed at high temperatures. The reaction layer between U-Mo and the Al matrix induces the volume expansion and degradation of the thermal properties of U-Mo/Al dispersion fuels[11]. It is important to investigate the reaction behavior between fuel particles and the matrix in the dispersion fuel.

In this study, high temperature annealing of U-Mo/Al dispersion fuels were carried out to analyze the reaction behavior of U-Mo/Al dispersion fuels. The growth rate of reaction layers with temperature and activation energy of the reaction layer growth of atomized U-Mo fuels were measured.

## 2. Experimental Procedures

U-10wt%Mo alloy was melted using a depleted uranium lump(99.9 wt%) and Mo (99.7wt%) by vacuum induction melting in a zirconia crucible, and then centrifugally atomized to U-10Mo alloy powders. The superheated molten U-Mo alloy was fed through a small nozzle onto a rapidly rotating graphite disk on a vertical axis. Liquid alloy droplets were then spread from the disk by a centrifugal force and cooled in an argon atmosphere. The atomized powder was collected in a container at the bottom of the funnel-shaped chamber. Meanwhile, an additional molten U-10Mo alloy was solidified in a graphite mold under a vacuum atmosphere. The as-cast U-10Mo ingot was heat-treated in a vacuum at 900 for 100 hrs to ensure compositional homogeneity, and then quenched to form the phase for the diffusion couple annealing between U-10Mo and Al sheet[12-14]. U-Mo powders of 75-90  $\mu\text{m}$  in diameter and pure Al powders of 20  $\mu\text{m}$  in diameter were mixed in a V-mixer with a rotation speed of 90 rpm for 1 hr and hot-extruded at 400°C with an extrusion ratio of 38:1. The growth behavior of reaction layers between U-Mo particles and the Al matrix was observed by the annealing of 10vol% U-10Mo/Al dispersion fuels at 500-550°C up to 36 hours in a vacuum sealed quartz tube. U-10Mo vs. Al diffusion couples were also annealed at temperature of 550°C for 5 hrs or 40 hrs in a vacuum atmosphere. The microstructure of U-Mo/Al dispersion fuels were characterized by scanning electron microscopy (SEM) and X-ray diffraction (XRD) techniques were used to identify the composition and crystal structure of the reaction layers. Concentration profiles of reaction layers in the diffusion couples were obtained by point-to-point counting techniques using a Jeol JXA8600 microprobe equipped with an energy dispersive spectrometer.

### 3. Results and Discussion

There are three kinds of intermetallic compounds such as  $UAl_2$ ,  $UAl_3$ ,  $UAl_{4.4}$  according to the U-Al phase diagram[15,16]. The crystallographic structure of  $UAl_3$  is the  $L1_2$  ordered structure (space group:  $Pm\bar{3}m$ ) with a lattice parameter of 0.426 nm and the  $UAl_{4.4}$  has a unit cell of body-centered orthorhombic (space group:  $Imma$ ) with lattice parameters of  $a=0.4397$  nm,  $b=0.6251$  nm, and  $c=1.3714$  nm[17,18].  $UAl_{4.4}$  forms a liquid phase at  $731^\circ\text{C}$  and  $UAl_3$  at  $1350^\circ\text{C}$  by peritectic reaction, respectively[15]. Annealed and quenched U-10Mo (wt.%) alloy correspond to the phase of U-21.6Mo(at.%) according to the U-Mo phase diagram[19].

Fig. 1 shows the micrographs of 10vol% U-10Mo/Al dispersion fuels after annealing for 40 and 90 min at  $550^\circ\text{C}$ . The bright-colored particles are atomized U-Mo alloy powders, the dark region is the Al matrix, and gray-colored reaction layers were formed between the U-Mo particles and the Al matrix. The thickness of the reaction layer increased with the annealing time.

When the annealing time was prolonged up to 25 hrs, only one reaction layer was observed at  $500^\circ\text{C}$ , whereas reaction layers divided into two or more intermediate phases after annealing at  $525^\circ\text{C}$  and  $550^\circ\text{C}$ . The reaction layers were designated as the internal part and the external part for composition analysis and the composition of U, Mo, and Al elements in the reaction layers obtained by energy dispersive spectroscopy are listed in Table 1. The compositions of the reaction layers at  $500^\circ\text{C}$  and the internal layer at 525 and  $550^\circ\text{C}$  were similar to  $(U,Mo)Al_3$  and the external layers at 525 and  $550^\circ\text{C}$  showed compositions corresponding to  $(U,Mo)Al_{4.4}$ . Lower temperature and shorter annealing time resulted in a single phase reaction layer in a U-10Mo/Al diffusion couple.  $UAl_{4.4}$  structured intermetallic phase may not form due to nucleation difficulties at lower temperatures, but can form at higher temperatures where the nucleation of the phase becomes activated.  $UAl_{4.4}$  structured intermetallic phase can appear only if an adjacent phase has a certain critical thickness due to a problem in the materials balance[20]. The growth kinetics of the  $UAl_{4.4}$  phase are known to be slow compared to that of the  $UAl_3$  phase and a phase based on the  $UAl_3$  structure is more stable than  $UAl_4$ [21,22].

Fig. 2 shows the relationship between the reaction layer thickness and annealing time with annealing temperature. The layer thickness values were obtained from the data corresponding to the selected annealing time when the  $UAl_3$  structured reaction phase is predominant for each temperature. Therefore the rate constant  $k$  for growth is related to diffusion in the  $UAl_3$  structured reaction layer. It has been reported that the growth of the reaction layer follows a parabolic rate law in the U/Al and  $U_3Si$ /Al system[23,24]. For the kinetics of solid-state reactions, the Jander's model and the Ginstling-Brounshtein model are mainly used as the diffusion controlled reaction in a sphere[25-29]. Jander's model has some weaknesses due to the oversimplifications for the rate of thickening of the reaction product. His analysis is expected to hold for only small values of the reacted fraction where the surface can be considered to be plane[25]. Ginstling and Brounshtein, however, began their derivation from

Fick's second law in the case of spherical symmetry[29]. Therefore, the Ginstling-Brounshtein model is known to be more soundly based than the Jander's model[26].

The reaction kinetics model given by Jander takes the form[27],

$$[1 - (1 - \alpha)^{1/3}]^2 = kt / r_0^2 \quad (1)$$

where  $\alpha$  is the reacted fraction at time t, k is the reaction rate constant, t is annealing time, and  $r_0$  is the initial particle radius. The reacted fraction,  $\alpha$ , is expressed as,

$$\alpha = 1 - \left(1 - \frac{x}{r_0}\right)^3 \quad (2)$$

where x is the reaction layer thickness and the reaction rate constant, k is expressed as,

$$k = k_0 \exp\left(-\frac{Q}{RT}\right) \quad (3)$$

where  $k_0$  is pre-exponential factor, Q is the activation energy for reaction layer growth, R is the gas constant, and T is annealing temperature.

The Ginstling-Brounshtein model which also describes a three dimensional diffusion process through the reaction layer is expressed as[28],

$$[1 - 2\alpha/3 - (1 - \alpha)^{2/3}] = kt / r_0^2 \quad (4)$$

Eq.(4) is transformed as a function of  $r_c$  ( $=r_0-x$ ), which is the radius of unreacted powder using eq.(2) as follows:

$$\left[1 + 2\left(\frac{r_c}{r_0}\right)^3 - 3\left(\frac{r_c}{r_0}\right)^2\right] r_0^2 = kt \quad (5)$$

Eq.(5) is expressed as a function of reaction layer thickness, x ( $= r_0 - r_c$ ) as follows:

$$x^2 \left(1 - \frac{2x}{3r_0}\right) = kt \quad (6)$$

In this study, The Jander's model and the Ginstling-Brounshtein model are compared with each other for describing the diffusion phenomena of spherical particles. The reaction layer thickness vs. annealing time relationship gives the reaction rate constant which is obtained from Fig. 2 and the linearity coefficients and the values of k for each models are listed in

Table 2. Whereas both models show good linearity at all three temperatures, the Ginstling-Brounshtein model gives the closer linear fit[29].

The activation energy of the reaction process was calculated using an Arrhenius plot according to each model as shown in Fig. 3. The activation energy obtained from the Jander's model is 277 kJ/mol and that from the Ginstling-Brounshtein model is 316 kJ/mol. Rhee et al reported that the activation energy for growth of reaction layers in a  $U_3Si/Al$  system was 220 kJ/mol in the temperature ranges from 510-670°C[24].

A diffusion couple experiment was carried out to investigate the formation of intermediate phases between the U-Mo alloy and Al. When annealed at 550°C for 5 hrs, three layers of intermediate phases were shown as shown in Fig. 4. Concentration profiles for diffusion couples were determined by electron probe microanalysis equipped with an energy dispersive spectrometer as shown in Fig. 5. Fig. 5(b) shows the concentration profiles of Al, Mo and U in the enlarged area focused on intermediate reaction layers as shown in Fig. 4(b). When annealed at 550°C for 40 hrs, three reaction layers were visible as shown in Fig. 6 and the concentration profile of each phase is similar to the one annealed at 550°C for 5 hrs as shown in Fig. 7. The L1 layer thickened much more than other reaction layers when the diffusion couple was annealed for 40 hrs. The composition of the intermediate layer L1 is similar to  $UAl_3$  and the layer L2 is similar to  $UAl_{4.4}$  considering the atomic fraction of Al as shown in Table 3. Whereas the compositions of L1 and L2 layer are similar to those of the internal and external reaction layers in U-10Mo/Al dispersion fuel, further crystallographic analysis is required because the layer, L3 is an unknown phase according to the phase diagram.

Interdiffusion between diffusion couples was investigated and interdiffusion fluxes and interdiffusion coefficient for the components in the intermetallic layers were determined by Dayananda[30,31]. The interdiffusion flux at any section,  $x$ , at a given time,  $t$ , is determined from the following equation:

$$\tilde{J}_i = \frac{1}{2t} \int_{C_i^+ \text{ or } C_i^-}^{C_i(x)} (x - x_0) dC_i \quad (7)$$

where  $C^+$  and  $C^-$  refer to the concentrations in the terminal alloys, and  $x_0$  is the location of the Matano plane. An integrated interdiffusion coefficient is calculated over a concentration range from  $C_i(x_1)$  to  $C_i(x_2)$  by

$$\tilde{D}_t^{\text{int}} = \int_{x_1}^{x_2} \tilde{J}_i dx \quad (8)$$

The integrated interdiffusion coefficients of U and Al were calculated on the basis of Eq.(8) for each reaction layer between the diffusion couples as shown in Table 4. Reliable values of the integrated interdiffusion coefficients of Mo could not be obtained due to little difference in composition between each layer. The integrated interdiffusion coefficients for the L1 layer of  $UAl_3$  structure are larger than those for other layers consistently with the relative thickness of the layer. The decreasing integrated interdiffusion coefficients for the L3 layer with time show that L3 phase is not stable as the adjacent phases grow[20]. The interdiffusion values with varying temperature can be used for the determination of activation energy of interdiffusion of U and Al in the reaction layers.

## 4. Conclusions

The growth rate and its activation energy of reaction layers of U-10Mo/Al dispersion fuels were obtained by three dimensional reaction kinetics models. The activation energies of the growth of  $UAl_3$  structured reaction layers were 277 kJ/mol based on Jander's model and 316 kJ/mol according to the Ginstling-Brounshtein model. Concentration profiles of reaction layers in U-10Mo vs. Al diffusion couples showed that three layers of intermediate phase formed. The integrated interdiffusion coefficients of Al and U for the  $UAl_3$  structured phase were larger than those for other phases and were increased with annealing time.

## Acknowledgements

The authors would like to express their appreciation to the Ministry of Science and Technology (MOST) of Korea for its support of this work through the National Nuclear R&D Project.

## References

1. J.L. Snelgrove, G.L. Hofman, C.L. Trybus, T.C. Wiencek, in: Proceedings of the 18th International Meeting on RERTR, Seoul, Korea, 1996.
2. J.L. Snelgrove, G.L. Hofman, M.K. Meyer, C.L. Trybus, T.C. Wiencek, Nucl. Eng. Des. 178 (1997) 119.
3. M.K. Meyer, T.C. Wiencek, S.L. Hayes, and G.L. Hofman, J. Nucl. Mater., 278 (2000) 358.
4. A. Gay, M. Belieres, in: Proceedings of the 20th RERTR meeting, Jackson Hole USA, 1997.
5. A. Travelli, in: Proceedings of the 22th International Meeting on RERTR, Budapest, Hungary, 1999.
6. A. Travelli, in: Proceedings of the 14th International Meeting on RERTR, Sao Paulo, Brazil, 1998.
7. R. C. Birther, C. W. Allen, L. E. Rehn, G. L. Hofman, J. Nucl. Mater., 152 (1989) 73.
8. C. K. Kim et al., in: Proceedings 14th International Meeting on RERTR, Jakarta, Indonesia, 1991.
9. T. Kato, K. Kusaka, Mater. Trans. JIM, 31 (1990) 362.
10. G. L. Hofman, J. Rest, J. L. Snelgrove, T. Wiencek, in: Proceedings 18th International Meeting on RERTR, Seoul, Korea, 1996.
11. S. Nazare, J. Nucl. Mater., 124 (1984) 14.
12. M.A. Dayananda and Y.H. Sohn, Scripta Mater., 35 (1996) 683.
13. R.V. Patil, G.B. Kale and P.S. Gawde, J. Nucl. Mater., 297 (2001) 153.

14. K. Bhanumurthy, R.V. Patil, D. Srivatsava, P.S. Gawde and G.B. Kale, *J. Nucl. Mater.*, 297 (2001) 220.
15. L.P. Lee and H.P. Leighly, Jr., *Metall. Trans. A*, 6 (1975) 135.
16. M.E. Kassner, P.H. Adler, M.G. Adamson, D.E. Peterson, *J. Nucl. Mater.* 167 (1989) 160.
17. R.E. Rundle and A.S. Wilson, *Acta Crystallogr.*, 2 (1949) 148.
18. O.J.C. Runnals and R.R. Boucher, *Trans. AIME*, 233 (1965) 1926.
19. B.S. Seong, C.H. Lee, J.S. Lee, H.S. Shim, J.H. Lee, K.H. Kim, C.K. Kim, V. Em, *J. Nucl. Mater.* 277 (2000) 274.
20. M.A. Dayananda and Y.H. Sohn, *Metall. Trans. A*, 30 (1999) 545.
21. D. Subramanyam, M.R. Notis, and J.I. Goldstein, *Metall. Trans. A.*, 16 (1985) 589.
22. I. Dahan, G. Kimmel, J. Sariel and S. Nathan, *Mater. Sci. Forum*, 133-136 (1993) 467.
23. G. Kimmel, A. Bar-Or and A. Rosen, *Trans. ASM*, 61 (1968) 703.
24. C.K. Rhee, S.I. Pyun and I.H. Kuk, *J. Nucl. Mater.* 184 (1991) 161.
25. R.E. Carter, *J. Chem. Phys.* 34 (1961) 2010.
26. J.H. Sharp, G.W. Brindley, and B.N. Narahari Achar, *J. Am. Ceram. Soc.* 49 (1966) 379.
27. W. Jander, *Z. Anorg. Allg. Chem.*, 163 (1927) 1.
28. A.M. Ginstling and V.I. Brounshtein, *J. Appl. Chem. USSR*, 23 (1950) 1327.
29. C.H. Lu and J.T. Lee, *Ceramics International*, 24 (1998) 285.
30. M.A. Dayananda, *Metall. Trans. A*, 14 (1983) 1851.
31. P.C. Tortorich and M.A. Dayananda, *Metall. Trans. A*, 30 (1999) 535.

Table 1. Compositions(at.%) of U, Mo, and Al in the reaction layers of U-Mo/Al dispersion fuels annealed for 25 hrs at temperature from 500 to 550°C. .

element \ temp.	500°C/25hr	525°C/25hr		550°C/25hr	
		internal layer	external layer	internal layer	external layer
U	19.5	20.5	11.2	18.0	13.8
Mo	4.1	3.8	3.7	4.9	2.9
Al	76.4	75.7	85.1	77.1	83.3

Table 2. The linearity coefficient (R) and reaction rate constant (k) of the reaction layer thickness vs. annealing time relationship according to the Jander's model and the Ginstling-Brounshtein model.

Annealing temperature (°C)	Jander's model		Ginstling-Brounshtein model	
	k (m <sup>2</sup> /hr)	R	k (m <sup>2</sup> /hr)	R
500	4.1	0.975	3.3	0.983
525	12.9	0.992	9.3	0.997
550	70.2	0.997	47.8	0.999

Table 3. Compositions of U, Mo, and Al in the reaction layers of U-Mo vs. Al diffusion couples annealed for 5 hrs and 40 hrs at temperature of 550°C.

element	composition in L1 layer (at.%)	composition in L1 layer (at.%)	composition in L2 layer (at.%)	composition in L3 layer (at.%)
U	5 hrs	17.8	15.1	5.3
	40 hrs	17.7	14.6	5.4
Mo	5 hrs	4.7	3.9	6.9
	40 hrs	4.7	3.8	6.3
Al	5 hrs	77.5	81.0	87.8
	40 hrs	77.6	81.6	88.3

Table 4. Integrated interdiffusion coefficients for reaction layers in the U-Mo vs. Al diffusion couples.

Reaction Layer	Temperature (°C)	Annealing time (h)	$\tilde{D}_U^{\text{int}}$ (m <sup>2</sup> s <sup>-1</sup> )	$\tilde{D}_{Al}^{\text{int}}$ (m <sup>2</sup> s <sup>-1</sup> )
L1	550	5	$7.1 \times 10^{-13}$	$9.1 \times 10^{-13}$
	550	40	$1.5 \times 10^{-12}$	$1.9 \times 10^{-12}$
L2	550	5	$1.1 \times 10^{-13}$	$1.4 \times 10^{-13}$
	550	40	$4.1 \times 10^{-14}$	$5.4 \times 10^{-14}$
L3	550	5	$4.0 \times 10^{-14}$	$8.8 \times 10^{-14}$
	550	40	$2.1 \times 10^{-15}$	$4.7 \times 10^{-15}$



Table 5. The density and uranium density of U-Mo/Al dispersion fuel with the volume fraction of U-Mo fuels.

fuel	Vol%	wt%	density (g/cm <sup>3</sup> )	uranium density (gU/cm <sup>3</sup> )
U-10Mo/Al	10	41.2	4.13	1.53
	30	73.0	7.00	4.60
	40	80.8	8.43	6.13
	50	86.3	9.86	7.66
U-10Mo			17.0	15.3
U <sub>3</sub> Si			15.5	14.6
U <sub>3</sub> Si <sub>2</sub>			12.2	11.3

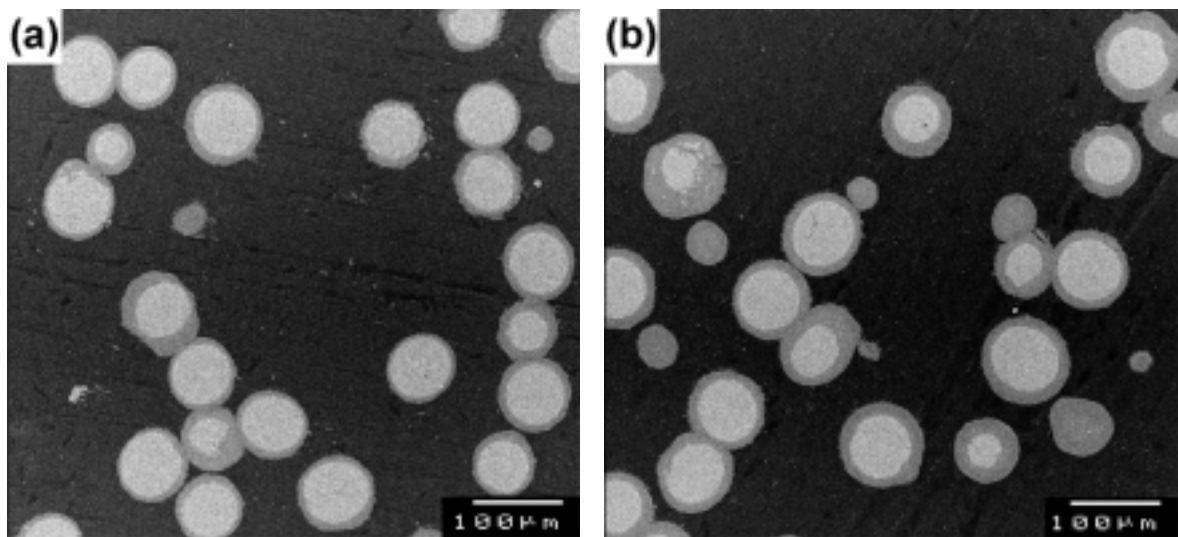
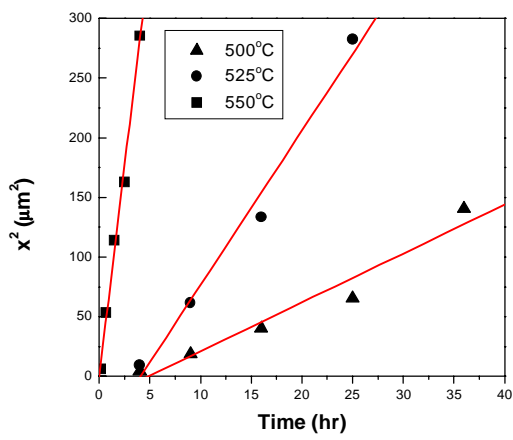
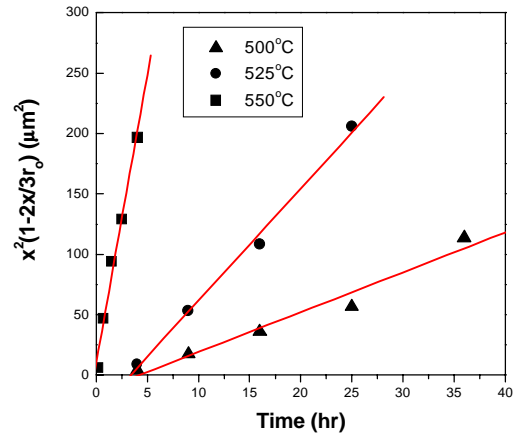


Fig. 1. The scanning electron micrographs showing the reaction layers in 10vol% U-Mo/Al dispersion fuels annealed for (a) 40 min and (b) 90 min at 550°C.

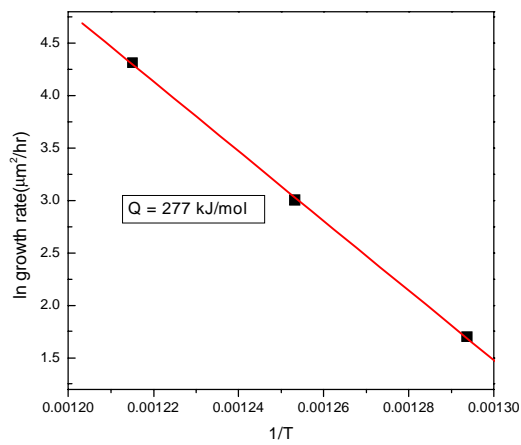


(a)

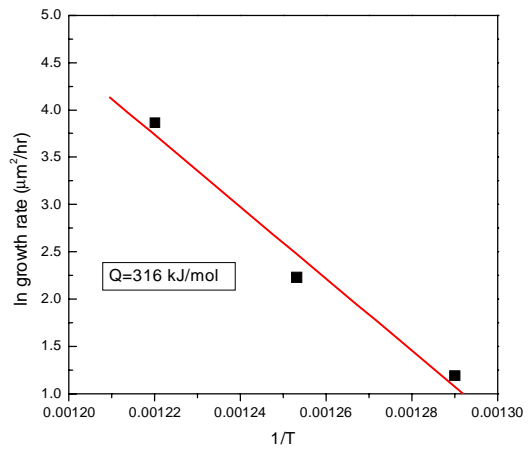


(b)

Fig. 2. The variation of thickness and reaction rate constant of the reaction layer obtained from (a) the Jander's model and (b) the Ginstling-Brounshtein model with increasing annealing time at 500, 525 and 550°C.



(a)



(b)

Fig. 3. The Arrhenius plot showing the activation energy according to (a) the Jander's model and (b) the Ginstling-Brounshtein model.

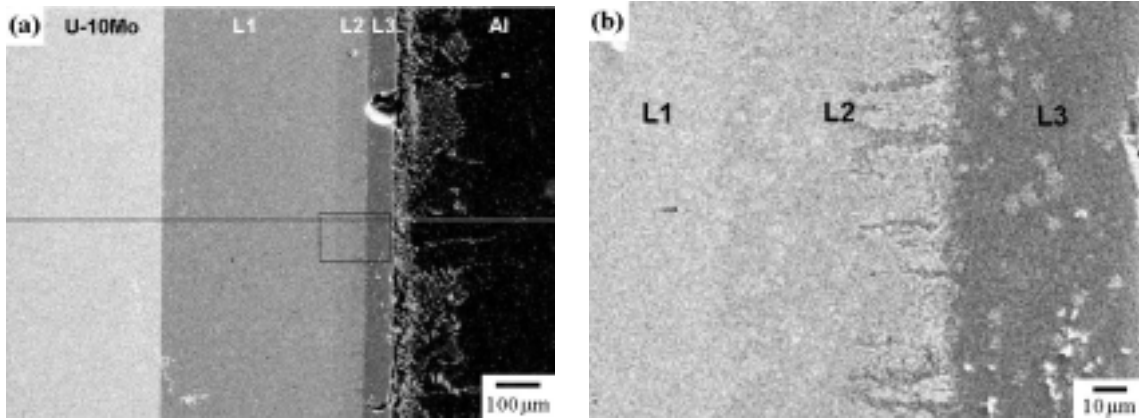


Fig. 4. The scanning electron micrographs showing (a) whole view of diffusion couple and (b) enlarged view especially focused on intermediate reaction layers after annealing of U-10Mo vs. Al diffusion couples at 550°C for 5 hrs.

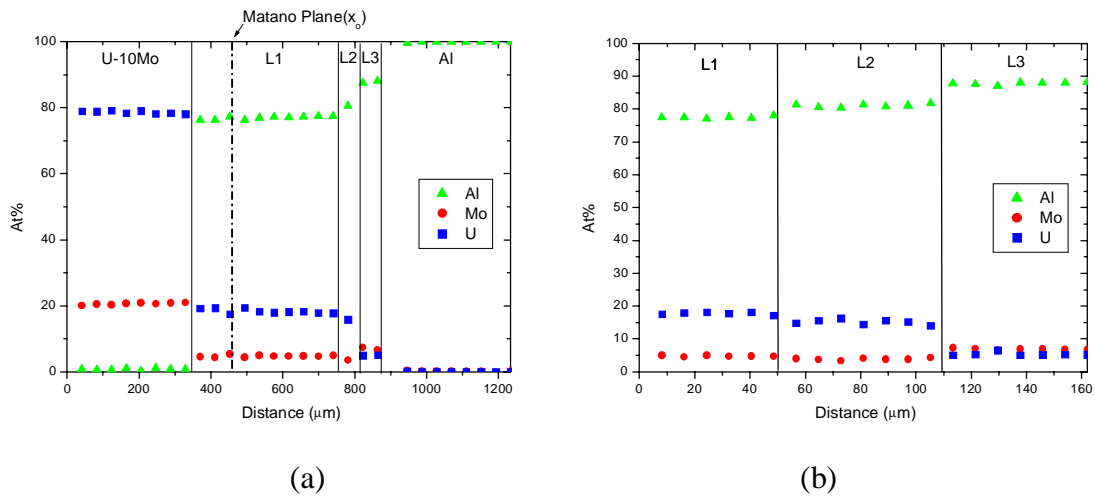


Fig. 5. The concentration profiles for U-10Mo vs. Al diffusion couples corresponding to (a) whole view of diffusion couple as shown in Fig. 4(a), and (b) enlarged view especially focused on intermediate reaction layers as shown in Fig. 4(b).

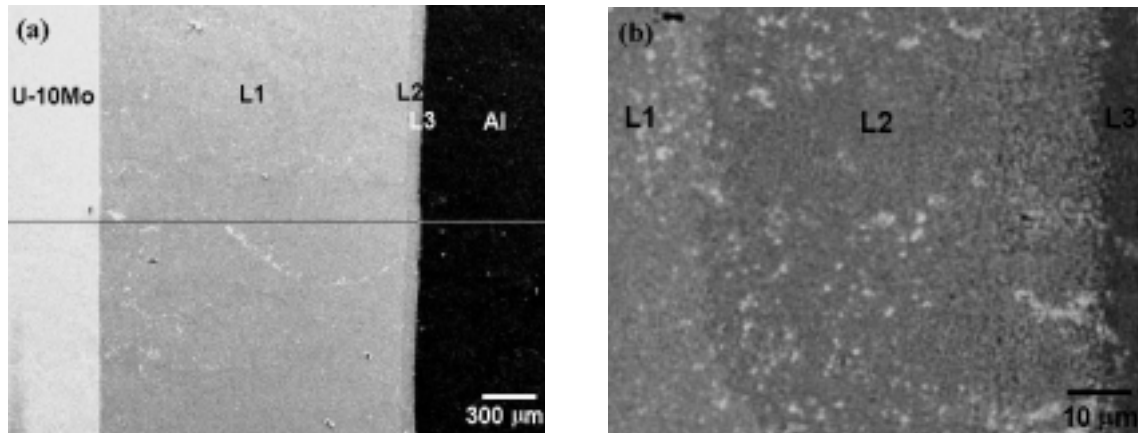


Fig. 6. The scanning electron micrographs showing (a) whole view of diffusion couple and (b) enlarged view especially focused on intermediate reaction layers after annealing of U-10Mo vs. Al diffusion couples at 550°C for 40 hrs.

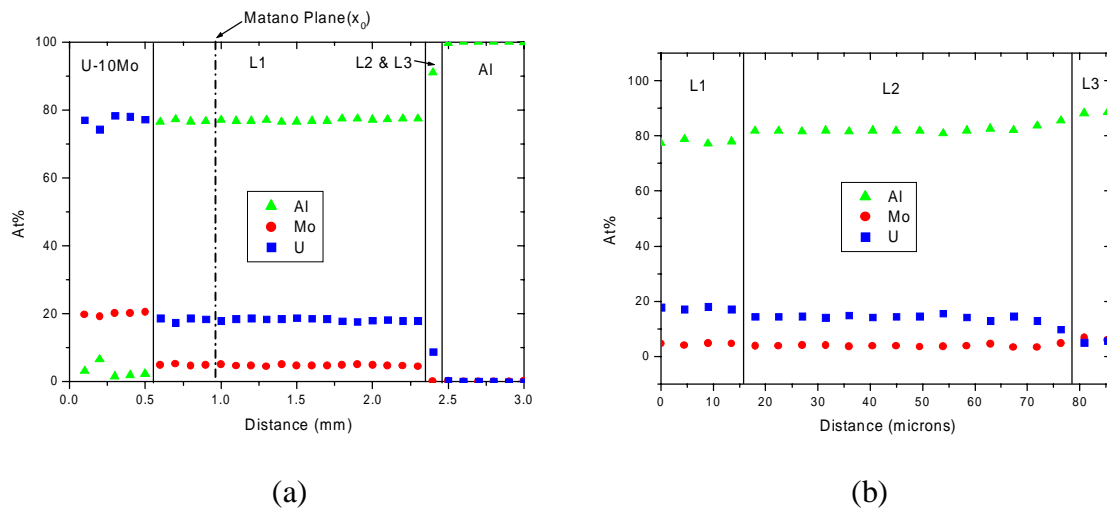


Fig. 7. The concentration profiles for U-10Mo vs. Al diffusion couples corresponding to (a) whole view of diffusion couple as shown in Fig. 6(a), and (b) enlarged view especially focused on intermediate reaction layers as shown in Fig. 6(b).